J. Electrochem. Sci. Eng. **15(4)** (2025) 2770; http://dx.doi.org/10.5599/jese.2770

Open Access : : ISSN 1847-9286
www.jESE-online.org

Original scientific paper

Performance of newly synthesized pyrimidine derivative as corrosion inhibitor: experimental and quantum chemical investigation

Halis Karataş[1], Mothana Ghazi Kadhim AlFalah[2,✉], Mehmet Izzettin Yilmazer[3], Murat Saracoglu[3], Zulbiye Kokbudak[1] and Fatma Kandemirli[4]

[1]*Erciyes University, Faculty of Science, 38039, Kayseri, Türkiye*
[2]*University of Al-Qadisiyah, Materials of Engineering Department, College of Engineering, 58002, Al-Qadisiyah, Iraq*
[3]*Erciyes University, Faculty of Education, 38039, Kayseri, Türkiye*
[4]*Kastamonu University, Faculty of Engineering and Architecture, 37150, Kastamonu, Türkiye*

Corresponding author: ✉mothana.kadhim@qu.edu.iq

Received: April 22, 2025; Accepted: June 19, 2025; Published: June 22, 2025

Abstract

*In this investigation, an alternative Schiff base with a pyrimidine ring was produced through the reaction of (1-amino-4-phenyl-2-thioxo-1,2-dihydropyrimidin-5-yl)(phenyl)methanone (**1**) with thiophene-2-carboxaldehyde. Structural verification of the resulting compound, designated (E)-phenyl (4-phenyl-1-(thiophen-2-ylmethyleneamino)-2-thioxo-1,2-dihydropyrimidin-5-yl)methanone, (PPTT), was accomplished by employing a number of spectroscopic methods, including ^{13}C-NMR, ^{1}H-NMR, and FTIR. Open-circuit potential, potentiodynamic polarization, linear polarization resistance, and electrochemical impedance spectroscopy were among the electrochemical methods used to evaluate the efficacy of PPTT as a corrosion inhibitor. After one hour of immersion, experimental data showed that PPTT functioned as a mixed-type corrosion inhibitor, attaining up to 83.8 % inhibition for 2 mM PPTT in 1 M HCl solution. Under these conditions, the corrosion current density dropped from 123.2 to 31.4 μA cm^{-2}. Surface adsorption of PPTT on mild steel in 1 M HCl followed the Langmuir adsorption isotherm, consistent with a negative Gibbs free energy value, indicating both chemisorption and physisorption. In addition, multiple quantum chemical parameters (electronegativity, E_{HOMO}, E_{LUMO}, chemical hardness, chemical softness) were calculated using Gaussian 09 to further elucidate the experimental observations.*

Keywords

Pyrimidine Schiff base; mild steel; corrosion resistance; electrochemical methods; quantum chemical calculations

Introduction

Metal corrosion prevention is crucial because its economic, structural and environmental consequences are extremely important [1,2]. Corrosion leads to degradation of the materials, thereby decreasing the life and mechanical characteristics of metallic structures that can result in catastrophic failure in a wide range of fields like construction, transportation, and energy. The economic consequences of corrosion are tremendous, with worldwide expenses in trillions of US dollars per year because of maintenance, repair, and replacement [3]. Furthermore, corrosion may lead to environmental hazards, for example, the spillage of hazardous substances from storage tanks and pipelines. Thus, corrosion-resistant surfaces play a vital role in enhancing the long-term dependability and stability of different metals and their alloys. Specifically, these protective coatings serve as barriers that prevent water and corrosive ions from interacting with the metal substrate. Effective corrosion inhibition techniques, such as surface treatments, electrochemical protection, and chemical inhibitors, minimize these hazards by extending the life of metals and reducing maintenance expenditures. Additionally, green corrosion inhibition techniques, such as environmentally friendly organic inhibitors and nanocoatings, conserve the environment while maintaining industrial performance [4].

Small quantities of compounds, corrosion inhibitors, are employed to reduce or stop corrosion. They function by minimizing the intense interactions between metal surfaces and their environment, thereby reducing the rate of deterioration. Among the several techniques used to control corrosion, the use of chemical compounds or naturally derived substances known as corrosion inhibitors is considered a fundamental strategy. In particular, researchers are investigating different types of inhibitors, including organic inhibitors and synthetic anticorrosive agents [5]. Among the various means of preventing corrosion, synthetic inhibitors are the most widely used because they are cost-effective to produce, highly effective, and easy to apply [6]. The effectiveness of these organic inhibitors stems from their composition, as they typically contain multiple heteroatoms and non-bonding electrons, along with π-electrons from extensive conjugation [6]. Heteroatoms, π-electrons, and non-bonding electrons serve as sites for adsorption during metal-inhibitor interactions. The adsorbed inhibitors provide a barrier that protects the metal surface, sheltering it from corrosive conditions and preventing breakdown. Organic inhibitors can attach themselves to the metal surface by electrostatic interactions or by sharing π-electrons and non-bonding with the metal's *d*-orbital or through a combination of both [7]. The efficiency of organic compounds as inhibitors of corrosion is ascribed to their high basicity and electron density, especially when enhanced with heteroatoms such as S, N, and O [8]. Heteroatoms affect the active sites, facilitating metal surface adsorption. Corrosion inhibition research and development are at the core of advancing materials science, ensuring more secure infrastructure, and supporting increased economic sustainability. Recent research has focused on the use of organic compounds containing heteroatoms, given their significant potential in preventing corrosion.

Thiophene-based compounds demonstrate considerable potential owing to the presence of the sulphur atom, which, with its relatively larger atomic size compared to oxygen, nitrogen, and carbon atoms, imparts distinctive characteristics to these molecules. The sulphur atom, along with other heteroatoms, contributes significantly to the inhibitory mechanism of organic compounds, significantly enhancing their efficacy in mitigating the corrosion of metallic substrates through adsorption and electron transfer processes [9].

With its unique nitrogen-rich structure closely bonding to metal surfaces to provide a protective barrier against rust, pyrimidine is a corrosion inhibitor of major relevance. Its eco-friendliness makes

it a safer alternative to harmful old inhibitors, and its adaptability allows scientists to change its structure for greater performance, making it innovative. Even in small amounts, it is also quite economical and efficient, a unique, eco-friendly way to defend against rust in the current time [10].

Pyrimidine forms a six-membered heterocyclic framework characterized by nitrogen atoms occupying the first and third positions in the ring system. The electronic structure of pyrimidine, particularly the delocalized π-electron cloud with non-bonding electron pairs on the nitrogen atoms, gives it a strong affinity for metal-surface interactions. This enables pyrimidine to function as a potent corrosion inhibitor *via* a donor-acceptor mechanism in which electron donation from nitrogen and π-electrons facilitates complexation with metal atoms. This interaction then leads to the formation of a robust and protective adsorption layer that reduces metal degradation [10]. A comprehensive review of the available literature reveals that various organic inhibitors containing a pyrimidine moiety have been systematically assessed for their efficiency in reducing metal corrosion in hydrochloric acid solutions. These studies have investigated various structural modifications of pyrimidine-based compounds to enhance their adsorption properties, optimize their interactions with metal surfaces, and improve their overall inhibitor performance. Results show the importance of pyrimidine derivatives as promising candidates for preventing corrosion in acidic conditions [11,12].

Arrousse *et al*. [13] conducted a detailed study on the corrosion inhibition potential of two newly synthesized pyrimidine-pyrazole derivatives for mild steel (MS) in 1 M hydrochloric acid medium. Their study showed significant inhibition efficiencies with 2-(((2,3-dihydro-1H-pyrazol-1-yl)methyl)amino)pyrimidine-4,6-diol achieving 77 % inhibition and 2-(bis((1H-pyrazol-1-yl)methyl)amino)pyrimidine-4,6-diol showing an even higher efficiency of 88 % at 1 mM concentration. The superior performance of these substances is due to their potent adsorption onto the metal surface, facilitated by electron-rich functional groups that enhance metal-inhibitor interactions and thereby effectively reduce corrosion [13].

Singh *et al*. [14] reported a study on the sustainable corrosion inhibitor capacity of two pyrimidine derivatives for N80 steel in an extremely corrosive setting, 15 % HCl medium. In this study, it was concluded that increasing the concentration of organic molecules caused the inhibition efficiency to increase gradually while decreasing the corrosion rate. This trend reaches a peak at 97 % inhibition efficiency for 8,8-dimethyl-5-*p*-tolyl-8,9-dihydro-1H-chromeno[2,3-d]pyrimidine-2,4,6(3H,5H,7H)-trione, and 94 % for 8,8-dimethyl-5-phenyl-8,9-dihydro-1H-chromeno[2,3-d]pyrimidine-2,4,6(3H,5H,7H)--trione, even at a relatively low concentration of 200 mg L^{-1}. The outcomes indicate that the enhanced inhibitor molecule surface coverage on the metal substrate is probably responsible for the inhibitory performance that was noticed. In aggressive acidic conditions, this enhanced adsorption efficiently prevents corrosive interactions and lessens metal corrosion by facilitating the creation of a more steady and safeguarding barrier [14].

The increasing importance of Schiff bases in preventing corrosion can be attributed to their facile synthesis from relatively low-cost starting materials and their environmentally friendly and low-toxicity properties. These advantageous properties make Schiff bases an attractive option for developing effective, sustainable corrosion inhibitors because they offer both economic and ecological benefits in addition to their excellent performance in protecting metals from corrosion. The high inhibitory performance of these compounds is primarily attributed to the strategic substitution of various heteroatoms (such as N, O, Cl, and Br) within their molecular structures and the contribution of delocalized π-electrons. In addition, the existence of the imine functional group (-C=N-) further enhances the corrosion inhibition efficiency. These structural features collectively

promote strong adsorption onto metal surfaces, improving the protective barrier and reducing metal degradation [15].

Nazir *et al.* [16] steered a complete study on the corrosion reduction potential of three ferrocene-based Schiff bases, each differing in the nature of their alkoxy substituents, for aluminium alloy in acidic media. Schiff bases containing -H, -OCH_3, and -OC_2H_5 substituents were produced and their ability to prevent corrosion performance was rigorously evaluated using both experimental techniques (such as electrochemical tests) and computational methods (such as density functional theory (DFT)). The results obtained from both approaches revealed a clear trend in inhibition efficiency, with the Schiff base containing the -OC_2H_5 substituent showing the highest inhibitory performance, followed by the -OCH_3 group, and finally the unsubstituted -H compound. This observed inhibition efficiency order can be explained by considering the electron-donating abilities of the substituents. The ethoxy group (-OC_2H_5) provides the highest electron density to the Schiff base structure through inductive and hyperconjugative effects, thus enhancing it can provide a protective barrier by adsorbing onto metal surfaces. In contrast, the methoxy group (-OCH_3) provides lower electron donation, reducing inhibition efficiency. The hydrogen atom (-H), which lacks any electron donation ability, contributes the least to the process of corrosion inhibition. The outcomes emphasize the significance of electronic effects in regulating the suppression of corrosion features of Schiff base compounds [16].

As potential corrosion inhibitors, heterocyclic compounds have been broadly utilized in corrosion inhibition studies [17]. Heterocyclic compounds that incorporate both sulphur and nitrogen atoms have much superior inhibitory efficacy to those with nitrogen or sulphur atoms [18].

In this context, in a study, a heterocyclic molecule PPTT containing three metal binding groups, namely pyrimidine, Schiff base and thiophene (Figure 1), was synthesized and characterized as reported in the literature [19], and subsequent corrosion inhibition studies were performed. Quantum chemical calculations based on DFT were performed to optimize the structure of the calculated molecule, several quantum chemical parameters, interpret the experimental findings and the inhibition mechanisms of the PPTT compound.

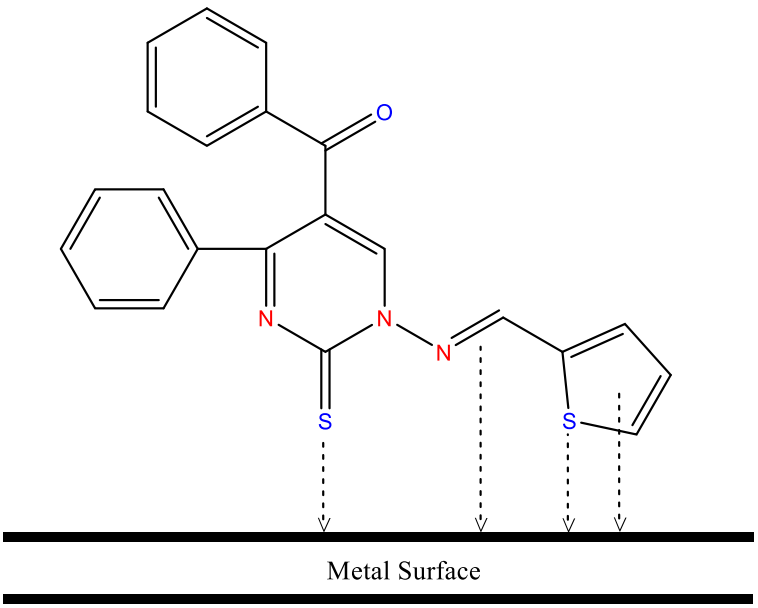

Figure 1. *Schematic illustration indicating adsorption mechanism of Schiff base on a metal surface*

Experimental

Chemical synthesis and characterization of PPTT

PPTT was prepared following a published procedure [19]. All other reagents and starting materials were commercially available. The reaction time and product purity were detected using plates and thin-layer chromatography (TLC) with a fluorescence indication at 254 nm. A digital Electrothermal 9100 apparatus was employed to measure melting points (mp). Infrared (IR) spectra were recorded using an ATR diamond cell in the 4000 to 600 cm^{-1} range. The ^{1}H-NMR measurements were conducted on a Bruker AM 400 MHz spectrometer.

The mixtures of PPTT (1 mmol) and thiophene-2-carboxaldehyde (1.2 mmol) were refluxed in 30 mL of ethyl alcohol when p-toluene sulfonic acid is present for 5 h (monitored by TLC). After cooling, the precipitate was filtered and crystallized in ethyl alcohol to afford Schiff base, (*E*)-phenyl (4-phenyl-1--(thiophen-2-ylmethyleneamino)-2-thioxo-1,2-dihydropyrimidin-5-yl)methanone, in good yields (80 %).

Corrosion testing

The mild steel (MS) rods used (0.8 cm diameter × 3 cm length) were purchased from a local supplier. Their chemical composition is approximately 0.18 % C, 0.0556 % Cr, 1.018 % Si, 0.699 % Mn, 0.0939 % Cu and 97.87 % Fe. The rods were machined into cylindrical test coupons and then used to assess corrosion behaviour in 1 M HCl, both with and without inhibitor. PPTT was made completely soluble in 1 M HCl solution using magnetic stirring for 2 h, followed by cleaning in an ultrasonic bath for 15 min. To facilitate testing, the back end of each coupon was implanted in epoxy resin and connected to a copper wire, exposing a 0.502 cm^2 area to the tested solutions. Surfaces were refined consecutively with silicon carbide papers (between 600 and 2500 grit) to achieve a reflective finish, then rinsed thoroughly with distilled water before air drying.

Electrochemical tests

A Compactstat electrochemical interface, instrument: B08024 (IVIUM, The Netherlands) electrochemical instrument was used for all electrochemical studies at ambient temperature. Potentiodynamic polarization (PDP) and linear polarization resistance (LPR) analyses were performed for mild steel samples immersed in 1 M HCl with or without inhibitor at a scan rate of 1 mV s^{-1}. The potential scan began at -0.7 V versus the corrosion potential (E_{corr}) and was increased to -0.2 V above E_{corr}, then reversed back down to E_{corr}. LPR measurements were taken within ±10 mV of the OCP. Electrochemical impedance spectroscopy (EIS) was applied to further characterize corrosion performance. EIS experiments were taken at the open-circuit potential, spanning 100 kHz down to 0.01 Hz with a 5 mV AC voltage amplitude. Tests were conducted in a 100 mL glass cell containing 1 M HCl solution, using an Ag/AgCl (3 M NaCl) electrode as the reference, a platinum wire as the counter electrode, and a mild steel sample as the working electrode (0.8 cm diameter, surface area of 0.502 cm^2). To make sure that the results were consistent, all of the electrochemical tests for PPTT were done at least three times. For data analysis, all plots were normalized to 1 cm^2.

Computational details

Calculations in quantum chemistry provide important information on the three-dimensional structure, reactivity, and bonding of molecules. By analysing key quantum chemical descriptors, it becomes possible to predict how effectively molecules inhibit corrosion by interacting with metal surfaces. FMO theory states that the adsorption sites on an inhibitory molecule that interacts with metal atoms can be identified [17]. The DFT approach is extensively used in corrosion science due

to its robust computational efficiency and accurate representation of molecular characteristics. The GaussView interface was utilized to construct the molecular structure, and the Gaussian 09 (Revision A.02) programme [20-22] was employed for DFT calculations. The geometry of the target molecule PPTT was optimized utilizing the 6-311++G(2d,2p) basis set and the B3LYP functional, considering both neutral and hydrated forms. From this optimized geometry, orbital energies for the HOMO and LUMO were obtained. Additional descriptors, including energy gap (ΔE), ionization potential (IP), electron affinity (EA), global electronegativity (χ), global hardness (η), global softness (σ), global electrophilicity (ω), total negative charge (TNC), dipole moment (DM), scaled electronic zero-point energy (SEZPE), and the fraction of electrons transferred (ΔN), were likewise determined. Equations (1) to (9) were utilized to determine the quantum chemical parameters via E_{HOMO} and E_{LUMO} [23,24].

$$\Delta E = E_{LUMO} - E_{HOMO} \quad (1)$$

$$IP = -E_{HOMO} \quad (2)$$

$$EA = -E_{LUMO} \quad (3)$$

$$\chi = \frac{IP+EA}{2} \quad (4)$$

$$\eta = \frac{IP-EA}{2} \quad (5)$$

$$\sigma = \frac{1}{\eta} = -\left(\frac{2}{E_{HOMO}-E_{LUMO}}\right) \quad (6)$$

$$\mu = -\chi = \left(\frac{E_{HOMO}+E_{LUMO}}{2}\right) \quad (7)$$

$$\omega = \frac{\chi^2}{2\eta} \quad (8)$$

$$\Delta N = \frac{\chi_{Fe}-\chi_{inh}}{2(\eta_{Fe}+\eta_{inh})} \quad (9)$$

To calculate the ΔN value, Fe_{χ} (global electronegativity for Iron) = 7 eV and Fe_{η} (global hardness for Iron) = 0 eV were used.

Monte Carlo simulation

Material Studio's 2017 adsorption locator employs Monte Carlo simulations (MCS) to look at how steel surfaces and inhibitor molecules come into contact with one another [24]. The simulations were done using an annealing method, with a time step of 1 fs and a total time of 100 ps. The size of the simulation box was 2.2×2.2×5.0 nm, with a super cell of 10×10 Fe (1 1 0) and a vacuum region of 8 nm. The system has a model of a Fe (110) surface and a model of $300H_2O + 4H_3O + 4Cl^- +$ PPTT. Using Ewald summation and an atom-based technique, we found the electrostatic potential and the van der Waals potential energy. The Forcite module finished the stage of optimising the geometry [24].

Equations (10) and (11) were used to calculate the adsorption energy (E_{ADS}) and binding energy ($E_{binding}$) of the examined PPTT on the iron surface:

$$E_{ADS} = E_{total} - E_{metal\ surface} - E_{inhibitor} \quad (10)$$

$$E_{ADS} = E_{binding} \quad (11)$$

where E_{total} , $E_{metal\ surface}$, and $E_{inhibitor}$ denote the total energy of the system, energy of the metal surface and energy of the PPTT, respectively.

Results and discussion

Characterization of the synthesized Schiff base (PPTT)

The initial synthetic step involved preparing PPTT, as shown in Figure 2. Subsequently, reacting PPTT with thiophene-2-carboxaldehyde in ethanol provided the novel Schiff base, PPTT, in an 80 % yield. Structural confirmation of the PPTT compound was carried out using spectroscopic analyses shown in Figures 3-5.

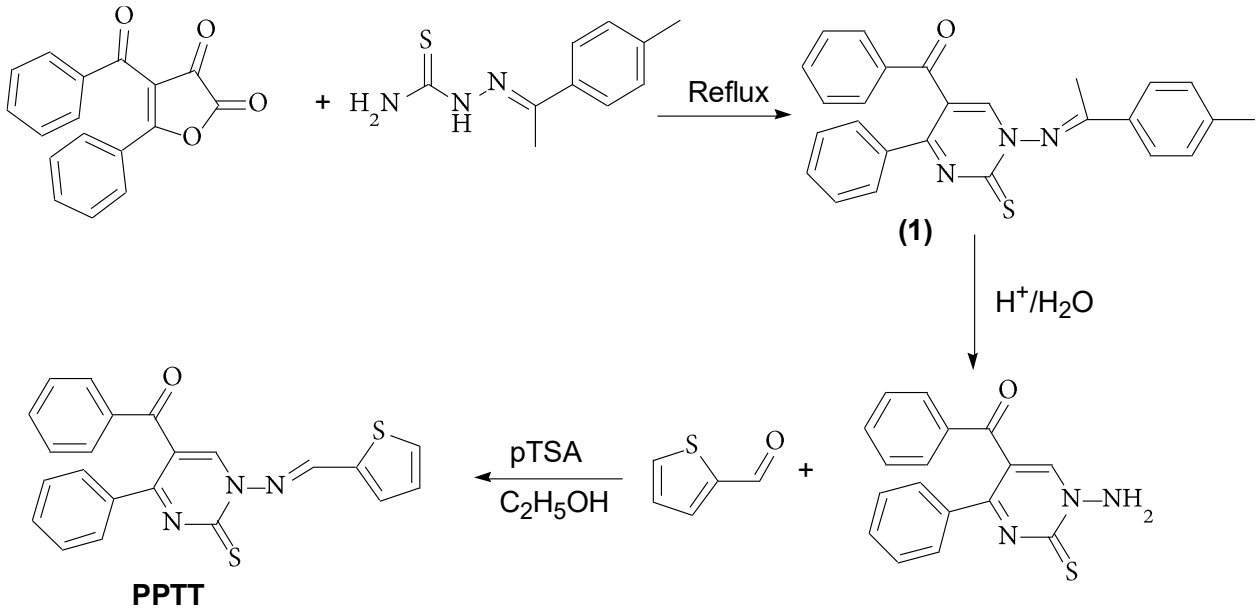

Figure 2. *Synthesis scheme of PPTT compound*

The structure of PPTT was characterized by FTIR (Figure 3), ^{13}C-NMR (Figure 4) and ^{1}H-NMR (Figure 5), and spectral techniques.

Yield: 70 %; mp: 207-208 °C; colour: yellow. FTIR: 3060.2 (aromatic C-H), 1648.0 (C=O), 1582.0, 1565.7 (C=N and C=C), 1219.1 cm^{-1} (C=S). ^{13}C-NMR (101 MHz, DMSO) δ 191.94, 176.18, 164.16, 146.83, 137.30, 136.71, 136.53, 136.07, 134.36, 134.31, 131.37, 130.32, 129.34, 129.22, 129.09, 128.89, 120.38. ^{1}H-NMR (400 MHz, DMSO) δ 9.12 (*s*, 1H), 8.92 (*s*, 1H), 8.46 - 7.25 (*m*, 13H).

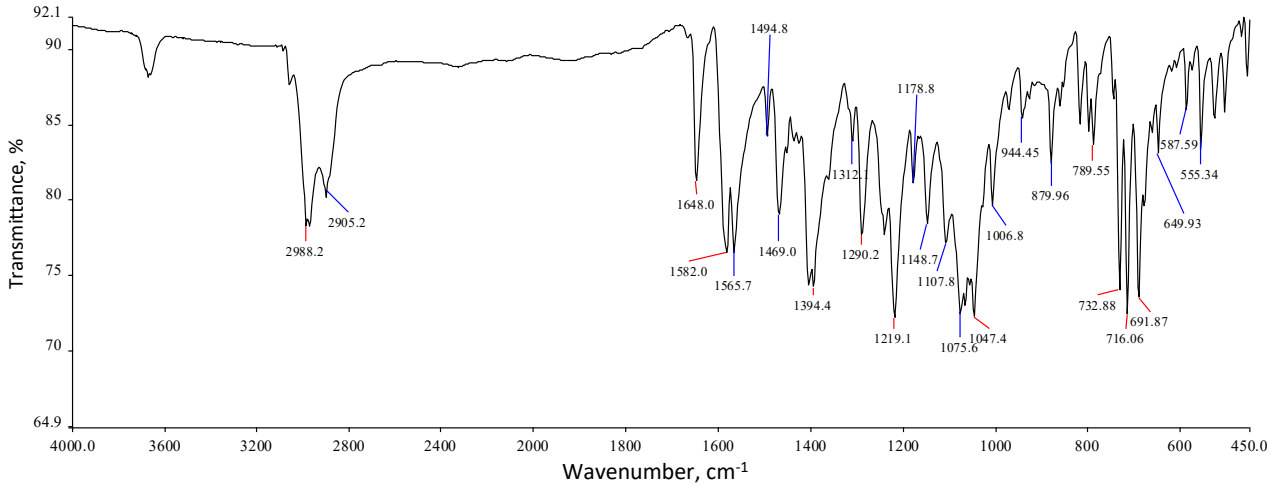

Figure 3*. FTIR spectrum of PPTT compound*

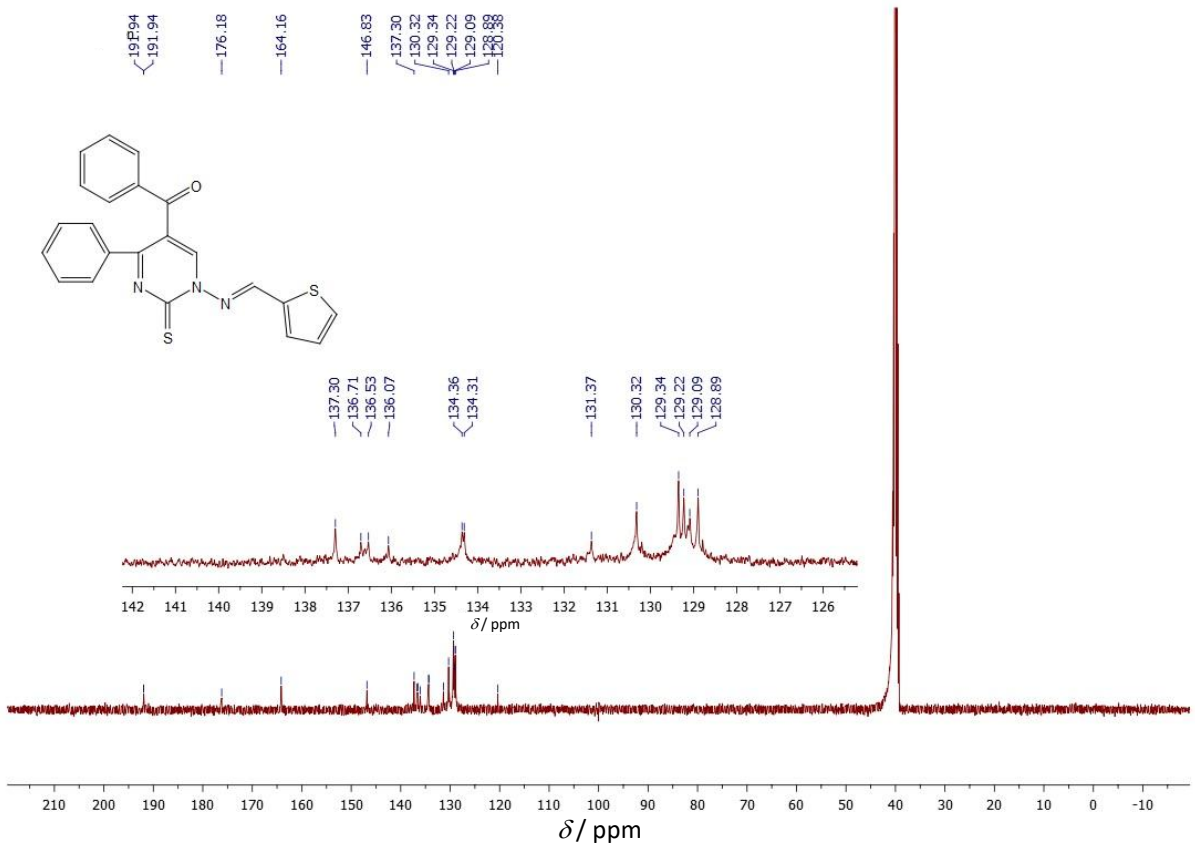

Figure 4. *^{13}C-NMR spectra of PPTT compound*

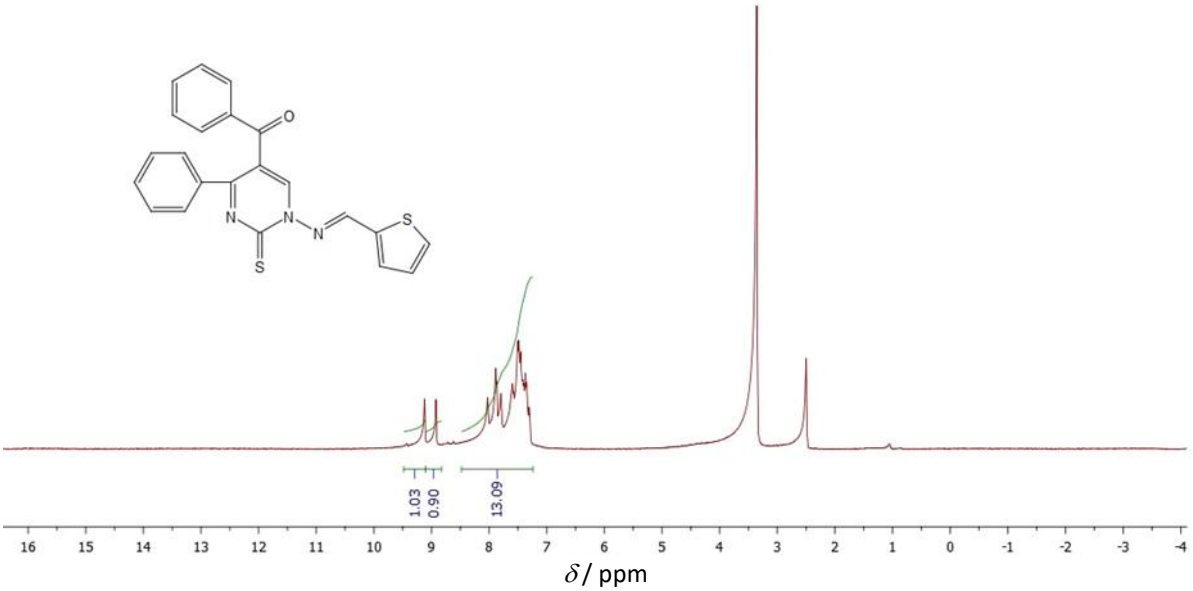

Figure 5. *^{1}H-NMR* spectra *of the PPTT compound*

In its ^{1}H-NMR spectrum, the proton associated with the N=CH group appeared as one peak at δ = 9.12 ppm in the downfield region, whereas multiplet signals between δ = 8.46 and δ 7.25 ppm represented aromatic protons. The ^{13}C-NMR spectrum had a notable resonance at δ = 191.73 ppm, indicative of a carbonyl group (C_6H_4C=O). FTIR results confirmed carbonyl (C=O) and thiocarbonyl (C=S) signatures at 1648.0 and 1219.1 cm^{-1}, respectively.

Electrochemical studies

Open circuit potential (OCP) values of mild steel were recorded for 60 minutes in both uninhibited and inhibitor-containing solutions. The PPTT results are displayed in Figure 6. At the onset of immersion in inhibitor-free acid, the OCP drifted negatively, presumably reflecting the steel's development of an oxide layer. Over time, increasingly negative potentials suggested that this oxide layer dissolved while iron chloride formed [25-27]. With the existence of the PPTT inhibitor, the final potential moved further negative, probably because inhibitor compounds interact with the reactive areas of mild steel and form a layer that protects the surface from external influences [23,28].

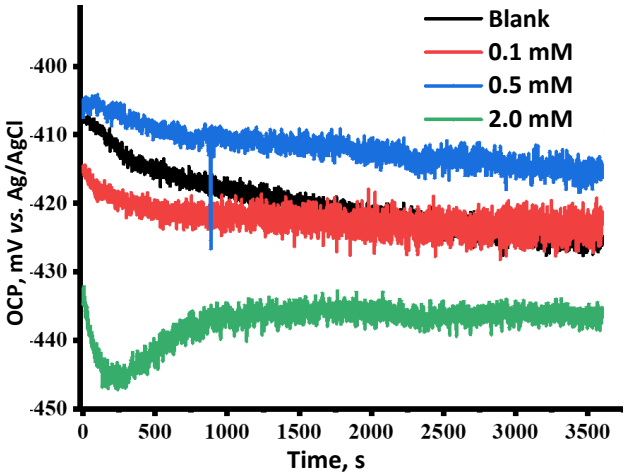

Figure 6. *Open circuit potential for mild steel immersion in 1 M HCl with and without the presence of PPTT at 298 K*

The corrosion inhibitor was examined using LPR and PDP tests. Figure 7 displays Tafel polarization curves of mild steel that was left exposed and steel that was treated with different concentrations of PPTT in a 1 M HCl solution for one hour. As the concentration of PPTT increased, the corrosion current decreased due to significant shifts in every branch, cathodic and anodic. This behaviour is attributed to the inhibitor adsorbing onto actively corroding metal areas, impeding Cl^- ions from damaging the steel.

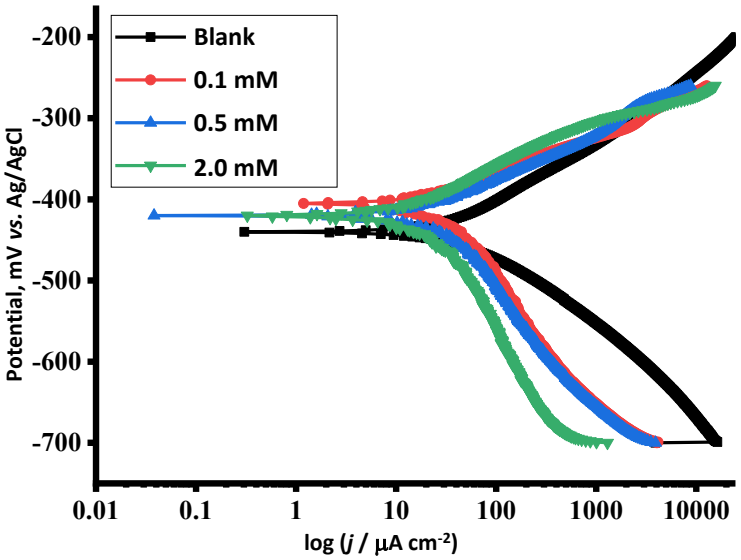

Figure 7. *PDP for mild steel immersion in 1 M HCl with and without presence of PPTT inhibitor at 298 K*

Table 1 lists all of the kinetic corrosion data for PPTT molecules that were determined, including E_{corr}, anodic (β_a) and cathodic ($-\beta_c$) Tafel slopes, corrosion current density (j_{corr}), surface coverage (θ), polarization resistance (R_{pl}), and inhibition efficiency (IE, %). Equations (12) and (13) were used to determine the IE_{PDP}, % and IE_{LPR}, % values [29]:

$$IE_{PDP} = \frac{j_{corr} - j_{corr(inh)}}{j_{corr}} 100 \quad (12)$$

$$IE_{LPR} = \frac{R_{pl(inh)} - R_{pl}}{R_{pl(inh)}} 100 \quad (13)$$

Table 1. *PDP and LPR parameters for MS immersion in 1 M HCl without and with the presence of corrosion inhibitor PPTT at 298 K*

C / mM	E_{corr} / mV	j_{corr} / μA cm^{-2}	$-\beta_c$ / V dec^{-1}	β_a / V dec^{-1}	θ	IE$_{PDP}$, %	R_{pl} / Ω cm^2	θ	IE$_{LPR}$, %
0 (blank)	440±2	123.2±0.2	0.103±0.003	0.080±0.004	---	---	208.33±3	---	---
0.1	406±3	49.6±0.1	0.159±0.001	0.060±0.002	0.5974	59.74	322.63±4	0.3542	35.42
0.5	420±2	48.4±0.3	0.174±0.006	0.042±0.001	0.6071	60.71	341.61±2	0.3901	39.01
2.0	462±1	31.4±0.2	0.195±0.004	0.086±0.003	0.7451	74.51	859.42±3	0.7576	75.76

Data in Table 1 show that with PPTT present, E_{corr} shifted slightly from -0.440 (blank) to -0.462 V, associated with the expanded inhibitor coverage. At the same time, j_{corr} dropped from 123.2 μA cm^{-2} (blank) to 31.4 μA cm^{-2} in the inhibited solution, highlighting PPTT's capacity to shield the steel from aggressive ions. The inhibition effectiveness progressively rose from 59.74 % at lower doses to 74.51 % at higher concentrations, and the polarization resistance results confirmed the Tafel data. The highest change in E_{corr} under inhibited circumstances was 0.02 V, which is why PPTT is classified as a mixed-type inhibitor [29].

As shown in Figure 8A, the Nyquist plots for MS in the absence of inhibitor features a depressed semicircle at almost all frequencies, which is indicative of surface roughness and inhomogeneity of the electrode surface.

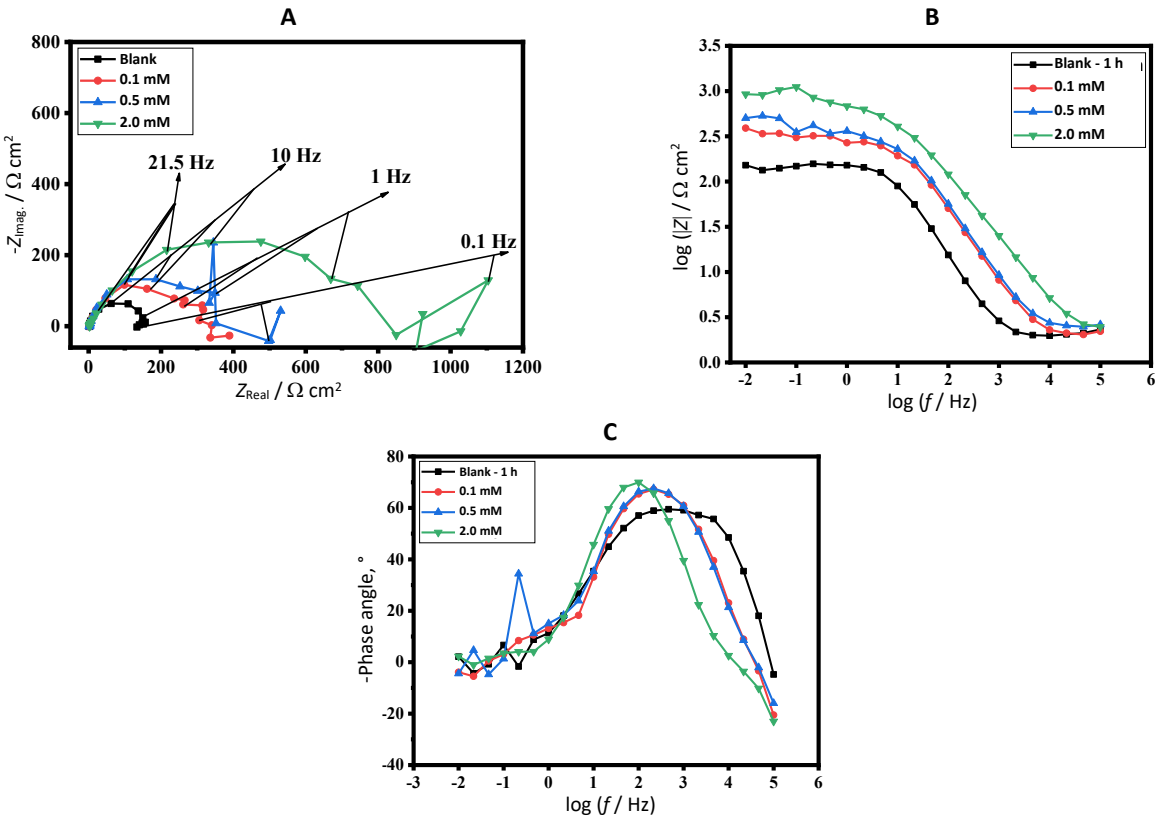

Figure 8. *Nyquist plots (A) and Bode plots (B-C) for MS immersion in 1 M HCl without and with the presence PPTT at 298 K*

When the PPTT inhibitor is present, the semicircle diameter grows, indicating an enhanced protective effect from inhibitor adsorption on the steel surface. In addition to semicircle diameters, the impedance magnitude ($|Z|$) at lower frequencies could be a key parameter for gauging inhibition efficiency. Figure 8B reveals that relative to uninhibited steel, $|Z|$ becomes larger at higher PPTT concentrations, attesting to the inhibitor's capacity to shield the steel against corrosion. Moreover, with PPTT addition, the phase angle curve (Figure 8(C)) is considerably elevated, which may stem from the relaxation caused by inhibitor molecule adsorption [24]. Overall, the EIS data closely align with results from OCP, LPR, and PDP measurements.

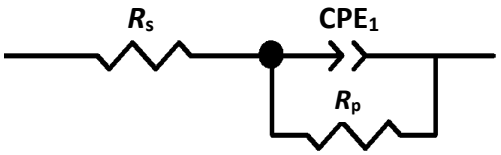

Figure 9. *Electrical equivalent circuit for MS corrosion without inhibitor and in the presence of PPTT inhibitor (R_S = Resistance of solution; R_P = Resistance of polarization; CPE_1 =Constant phase element)*

Parameters of electrochemical impedance spectroscopy (EIS) for PPTT, derived from fitting the electrical equivalent circuit in Figure 9 to impedance spectra in Figure 8, are provided in Table 2. Using Equation (14), corrosion inhibition efficiency (IE) was determined according to [30]:

$$IE_{EIS} = \frac{R_{P(inh)} - R_P}{R_{P(inh)}} 100 \quad (14)$$

Table 2. *EIS parameters of MS immersed in 1 M HCl solution with and without the presence of corrosion inhibitor PPTT at 298 K*

Concentration, mM	R_S / Ω cm^2	R_p / Ω cm^2	CPE_1, μF cm^{-2} s^{n-1}	*n*	IE, %
0.0 (blank)	1.03±0.01	145.02 ±2	351.15 ±2	0.84 ±0.03	---
0.1	1.01±0.03	340 ±1	177.76 ±3	0.87 ±0.01	57.34
0.5	1.15±0.02	500 ±3	139.96 ±1	0.89 ±0.02	71.00
2.0	1.05±0.02	896.09 ±4	112.89 ±2	0.91 ±0.04	83.81

Adsorption isotherm

The process of inhibitor molecules adhering to the metallic surface is an essential component of corrosion inhibition. Adsorption mechanism is frequently described by popular models such as Langmuir (Figure 10A), Frumkin (Figure 10B), and Temkin (Figure 10C) isotherms. The Langmuir isotherm, which is described by the following equation, was the best fit in the current investigation:

$$\frac{C_{inh}}{\theta} = \frac{1}{K_{ads}} + C_{inh} \quad (15)$$

where C_{inh} is the inhibitor-concentration, θ is the level of surface coverage by inhibitor, and K_{ads} is the equilibrium constant of adsorption.

PPTT's adsorption follows the Langmuir isotherm, as shown by the estimate of the relation coefficient ($R2$). The obtained plot of C_{inh}/θ *vs.* inhibitor fixation (C_{inh}) (Figure 10 (A)) is straight-forward and illustrates the Langmuir adsorption isotherms material. This $R2$ estimate also shows that the compound's atoms formed a layer of monomolecular on the terminal surface [31].

To quantify the adsorption free energy ($-\Delta G_{ads}$), the following equation was used:

$$\Delta G_{ads} = -RT \ln(55.5\, K_{ads}) \quad (16)$$

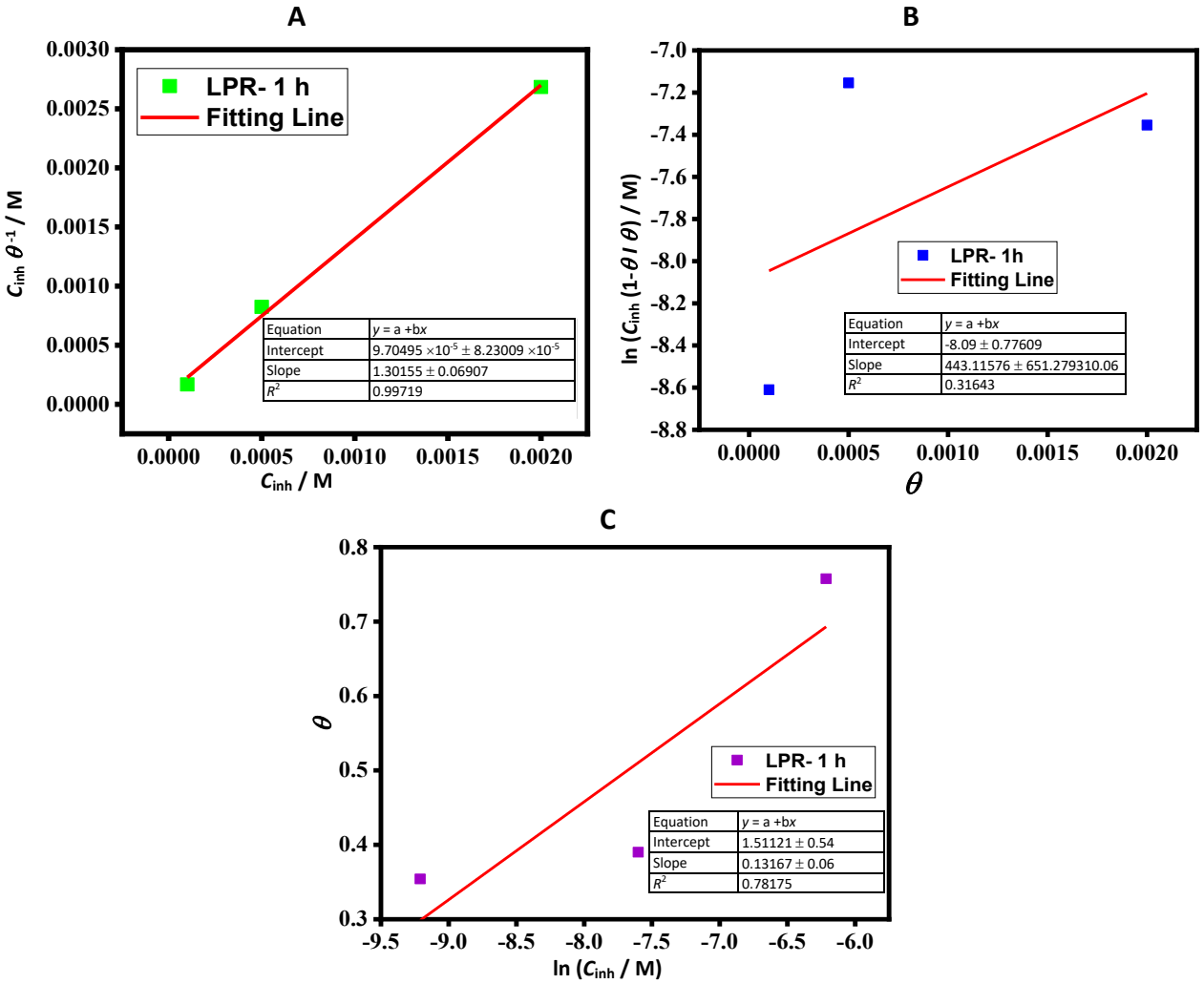

Figure 10. *Langmuir (A), Frumkin (B) and Temkin (C) adsorption isotherms for the MS surface*

The values of ΔG_{ads} around -20 kJ mol^{-1} indicate full electrostatic interaction (physisorption) while -40 kJ mol^{-1} or more negative values represent chemical interaction. The determined value of -32.1 kJ mol^{-1} suggests that the mild steel surface and PPTT inhibitor interact *via* mixed chemisorption and physisorption [32,33].

Density function theory calculations

Under the framework of frontier molecular orbital (FMO) theory, the chemical reactivity of a compound is largely dictated by interactions between its HOMO and LUMO. Figure 11 depicts the charge density distributions of both the HOMO and LUMO for the neutral and aqueous forms of the target molecule.

Inhibitor performance is closely tied to E_{HOMO}, as a higher E_{HOMO} indicates an enhanced capacity to donate electrons to a metal's empty d-orbital. Conversely, E_{LUMO} characterizes the capacity of the inhibitor to take electrons—lower E_{LUMO} values imply that electron acceptance is energetically more favourable [34]. Consequently, molecules featuring both one high E_{HOMO} and one low E_{LUMO} tend to form stronger adsorption layers on metal surfaces, yielding superior corrosion inhibition. For the investigated molecule, E_{HOMO} was determined to be -5.774 eV for the neutral form and −6.212 eV under aqueous conditions (Figure 11), suggesting that its electron-donating properties are more pronounced in the neutral phase. Moreover, molecules with smaller E_{LUMO} values, such as −2.610 eV (neutral) and

−2.714 eV (aqueous), typically facilitate more robust adsorption [35-39]. This reduced E_{LUMO} may account for the promising corrosion inhibition performance observed.

The parameter Δ*E* is instrumental in assessing the stability and chemical reactivity of inhibitor molecules. According to Murulana *et al.* [38], a higher Δ*E* value corresponds to greater molecular stability and thus lower reactivity, whereas a lower Δ*E* value signifies heightened reactivity. Notably, as ΔE decreases, the affinity between the inhibitor and the metallic surface increases, leading to stronger corrosion inhibition [38]. Based on these Δ*E* findings, the neutral molecular form is predicted to offer better inhibition (Figure 11).

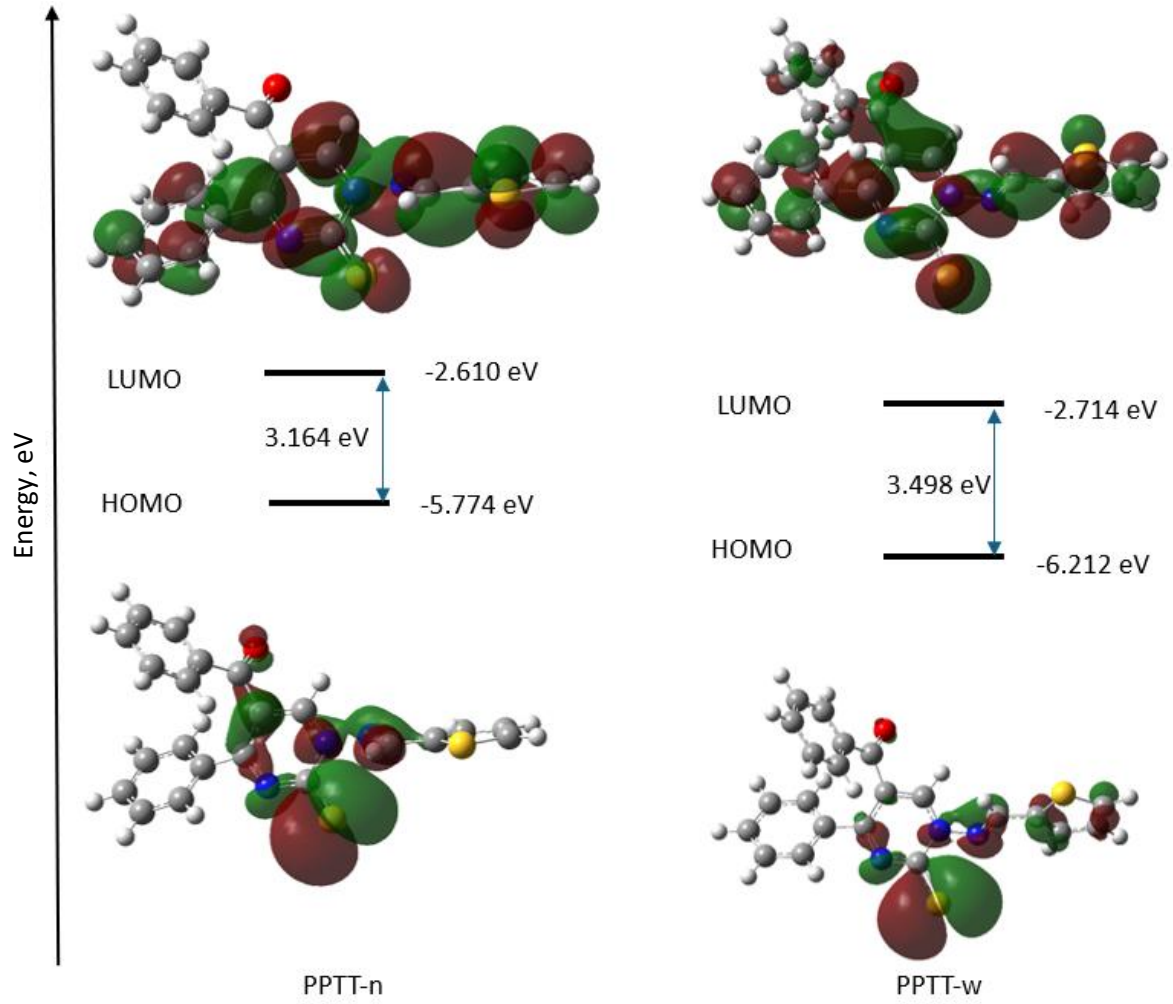

Figure 11. *Frontier molecular orbitals (HOMO and LUMO) and HOMO-LUMO energy gaps for neutral (n) and water (w) phases of PPTT*

Ionization potential (IP) represents another pivotal measure of chemical reactivity. A higher IP implies increased inertness and stability, whereas a lower IP indicates elevated reactivity [34]. The IP results suggest that, for PPTT, the neutral form should deliver superior inhibitory efficiency (Table 3).

Chemical hardness (η) reflects how resistant an atomic or molecular electron cloud is to polarization. Regarding the principle of maximal hardness, a chemical species naturally tends to assume a configuration with maximum hardness, meaning a lower η value correlates with stronger corrosion inhibition [40]. Chemical softness (σ), conversely, quantifies the polarizability of the molecule and is inversely related to hardness. According to [41] and [42], softness scales with the polarizability cube root. Additionally, the minimum polarizability principle posits that softer molecules can more readily donate electrons to metallic surfaces, thereby enhancing their

anticorrosion performance. In fact, molecules boasting the highest softness display more pronounced adsorption onto metal surfaces. Based on the determined hardness and softness parameters, the neutral molecular form is again deemed to function as a corrosion inhibitor more effectively than the aqueous form (Table 3).

Table 3. *The quantum chemical parameter values computed for neutral (PPTT-n) and water (PPTT-w) phases of PPTT compound*

	PPTT-n	PPTT-w		PPTT-n	PPTT-w
IP, eV	5.774	6.212	ω / eV	5.553	5.694
η / eV	1.582	1.749	μ / eV	-4.192	-4.463
σ / eV^{-1})	0.632	0.572	TNC, e	-5.657	-8.111
χ / eV	4.192	4.463	SEZPE, eV	-51245.080	-51245.703
DM, D	3.461	9.234	ΔN	2.222	2.219

Per the principle of electronegativity balancing (PBE), when an inhibitor and a metal come into proximity, electrons stream from the species with lower electronegativity to that with higher electronegativity until their chemical potentials or electronegativities equilibrate [43]. Hence, an inhibitor's electronegativity dictates the percentage of electrons that pass through the inhibitor and land on the metal surface. In general, an inhibitor with reduced electronegativity tends to donate electrons more readily, resulting in enhanced corrosion mitigation [44]. As indicated in Table 3, the inhibitor under investigation has electronegativity (χ) values of 4.192 eV in the neutral state and 4.463 eV in the aqueous form, implying that the neutral species is likely more effective at corrosion inhibition.

Another parameter influencing the performance of organic inhibitors is the dipole moment (DM). The correlation between DM and inhibitor efficacy remains a point of debate [45]. Some studies argue that DM does not correlate directly with inhibition [34], while others suggest that inhibitors become more potent as DM increases [45,46]. It has also been noted that greater DM can facilitate electron transfer [43,47]. As shown in Table 3, DM values support the conclusion that the neutral state of PPTT acts as a more efficient inhibitor, presumably because higher dipole moments promote enhanced interactions between dipoles with the charged metal surface, thus improving molecular adsorption [48,49].

Recent literature indicates that the global electrophilicity index (ω) can be used to characterize a molecule's inhibitory performance [46,47,50]. It has been proposed that compounds exhibiting higher electrostatic parameters perform poorly at inhibiting corrosion, whereas those with lower electrostatics or higher nucleophilicity show better protection [48,51]. Another metric is the chemical potential (μ): a lower μ signifies a more nucleophilic species with greater reactivity. By examining ω and μ values, it becomes evident that the neutral form of PPTT offers better mild steel protection than the aqueous form. Also noteworthy is the total negative charge (TNC), determined by summing all negative charges in the molecule, which can shed light on how effectively the inhibitor interacts with the metal. Higher TNC typically implies stronger adsorption [46]. Additionally, a molecule with a higher SEZPE value is more prone to electron donation and exhibits greater stability [52]. According to Table 3, the energetic values of PPTT in both neutral and aqueous phases are roughly comparable, further highlighting the favourable properties of the neutral species for corrosion inhibition.

Electrostatic potential (ESP) is a key indicator of the electrophilic and nucleophilic regions within a molecule, and it serves as a foundational tool for assessing molecular reactivity. DFT methods enable precise generation of ESP maps [53]. On these maps, the areas most prone to nucleophilic attack

appear in blue (positively charged), whereas red denotes the electrophilic domains (negatively charged). Figure 12 illustrates the ESP distributions for PPTT in both neutral and aqueous environments.

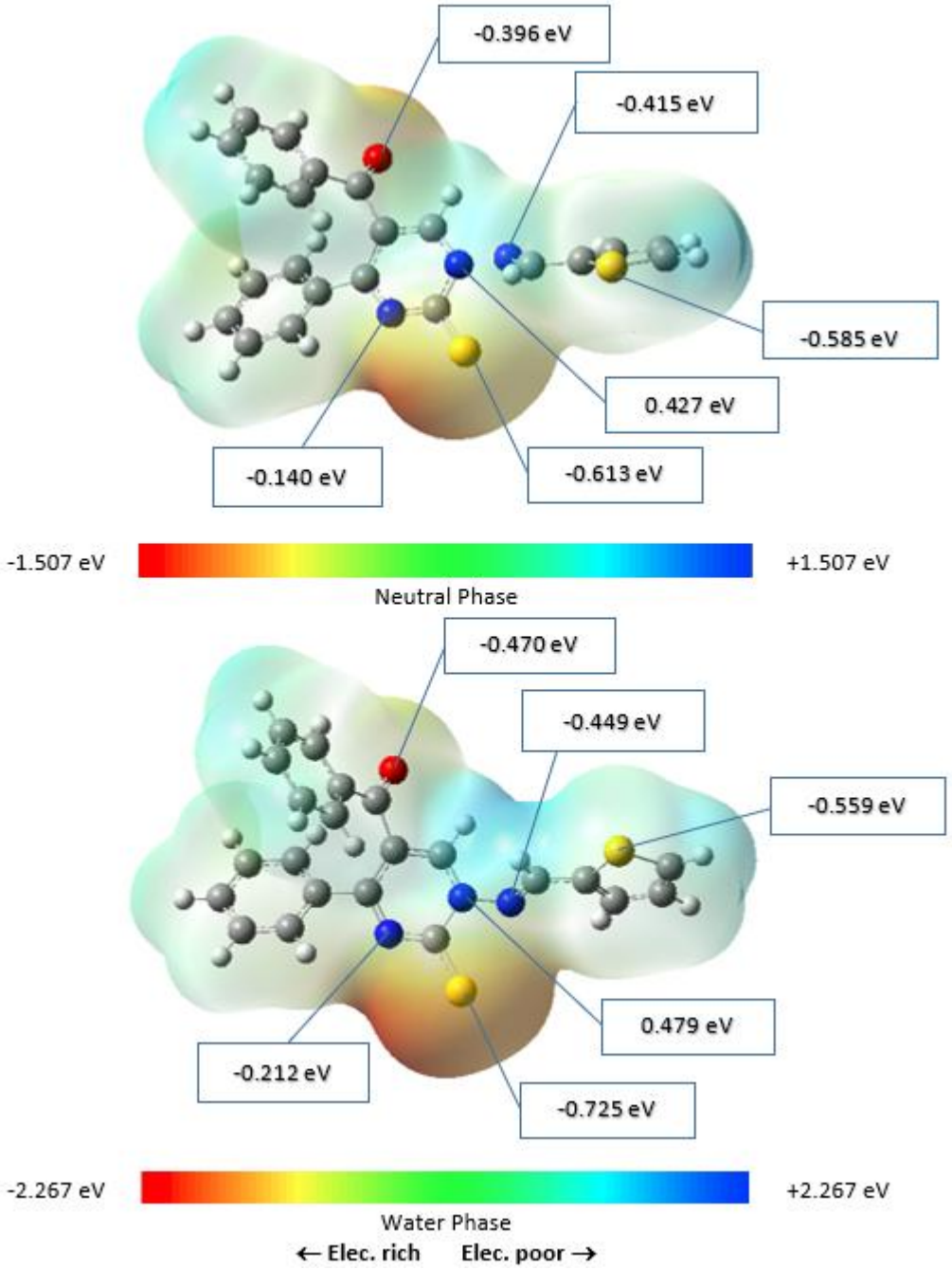

Figure 12. *The ESP surfaces for the neutral and water phases of molecule PPTT*

Notably, in Figure 12, the red coloration is particularly pronounced around the sulphur, nitrogen, and oxygen centres, suggesting that these sites favour the creation of covalent bonds with iron. d-orbitals. Therefore, the electron density surrounding these heteroatoms in the aqueous phase appears even higher than in the neutral phase. In general, a smaller ΔE (Figure 11) corresponds to stronger inhibition efficacy, elevated surface adsorption, and greater ease of molecular polarization. Another important parameter is the fraction of transferred electrons (ΔN), which provides insight into the inhibitor's performance. Empirical evidence shows that inhibition efficiency tends to rise when $\Delta N < 3.6$, with PPTT exhibiting ΔN values of 2.222 eV in the neutral form and 2.219 eV in the aqueous form [20,24,54].

Monte Carlo simulation

Figure 13 shows that the inhibitor has substantially more stable low-energy adsorption properties. The nitrogen and sulphur atoms have the most active sites for adsorption. To maximize surface coverage and contact, the PPTT molecule adheres to the metal surface in a virtually umbrella-like configuration, hence promoting robust interaction within the adsorbate/substrate system. The PPTT being studied is expected to stick to the metal surface, creating thick, water-repelling barriers against corrosion. Eads's finding was predicated on the mean adsorption energy of the resultant equilibrium configurations. For Fe (110) surfaces, the E_{ads} value we got is -482.92 kJ/mol. The adsorption energies are negative, which means that spontaneous adsorption is likely. Consequently, the theoretical computation performed in our work offers a precise explanation for the observed experimental phenomenon [24].

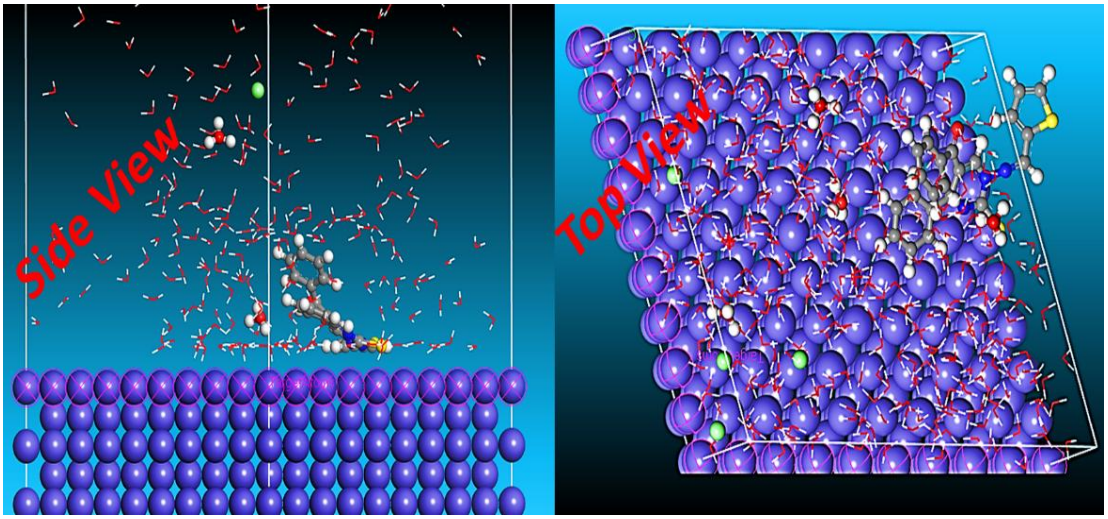

Figure 13. *Side view and top view for adsorption of molecule PPTT on Fe (110) surface*

Conclusions

In this research, an 80 % yield of a novel pyrimidine-based Schiff base (PPTT) was achieved, and the resulting compound was characterized *via* FTIR, ^{1}H-NMR, and ^{13}C-NMR methods. Beyond synthesizing PPTT, its corrosion inhibition properties were examined by means of multiple electrochemical techniques, specifically open-circuit potential, potentiodynamic polarization, linear polarization resistance, and electrochemical impedance spectroscopy, across various concentrations. In addition, quantum chemical evaluations were performed on the neutral and aqueous states of PPTT to complement the experimental findings. The inhibitor's adsorption behaviour adhered to the Langmuir isotherm, and the negative Gibbs free energy (ΔG_{ads}) demonstrated that PPTT functions as a mixed-type inhibitor.

DFT calculations and Monte Carlo simulations confirmed the establishment of a stable barrier on mild steel. Analyses of E_{HOMO}, E_{LUMO}, ΔE, IP, η, σ, χ and ω collectively showed that both electron donation and inhibition potential were enhanced for the neutral form of PPTT when compared to its aqueous form. Electrostatic potential analyses likewise support the conclusion that the neutral phase outperforms the water phase in corrosion inhibition.

Acknowledgements*: The computers used for quantum chemical calculations were allocated by the Erciyes University data centre.*

Ethical approval: *Ethics committee report was not required because live subjects were not used.*

Competing interests*: There are no personal conflicts of interest between the authors for this article.*

Author Contributions: *Conceptualization, M.S., Z.K., M.G.K.A. and F.K.; data curation, M.S., M.I.Y., Z.K. and F.K.; formal analysis, M.S. and M.I.Y.; investigation, M.S., M.G.K.A., M.I.Y., H.K., Z.K. and F.K.; methodology, M.S., M.I.Y., M.G.K.A., H.K., Z.K. and F.K.; resources, M.S., H.K., M.G.K.A. and M.I.Y.; software, M.S. and M.I.Y.; supervision, M.S, and F.K.; Synthesis and characterization, H.K, Z.K; validation, M.S., Z.K. and F.K.; writing—original draft preparation, M.S., H.K., M.G.K.A., Z.K. and F.K.; writing—review and editing, M.S., H.K., M.I.Y., M.G.K.A. and F.K.; visualization, M.S., M.I.Y. and H.K.; All authors have read and agreed to the published version of the manuscript.*

Funding: *This study was supported by Erciyes University projects coded: FBA-07-21 and FHD-2020-10349.*

Availability of data and materials: All the research data are available from the authors.

References

[1] A. Al-Amiery, W. N. R. Wan Isahak, W. K. Al-Azzawi, Sustainable corrosion Inhibitors: A key step towards environmentally responsible corrosion control, *Ain Shams Engineering Journal* **15** (2024) 102672. https://doi.org/10.1016/j.asej.2024.102672

[2] R. Bender, D. Féron, D. Mills, S. Ritter, Ralph Bäßler, D. Bettge, I. D. Graeve, A. Dugstad, S. Grassini, T. Hack, M. Halama, E. H. Han, T. Harder, G. Hinds, J. Kittel, R. Krieg, C. Leygraf, L. Martinelli, A. Mol, D. Neff, J.O. Nilsson, I. Odnevall, S. Paterson, S. Paul, T. Prošek, M. Raupach, R. I. Revilla, F. Ropital, H. Schweigart, E. Szala, H. Terryn, J. Tidblad, S. Virtanen, P. Volovitch, D. Watkinson, M. Wilms, G. Winning, M. Zheludkevich, Corrosion challenges towards a sustainable society, *Materials and Corrosion* **73** (2022) 1730-1751. https://doi.org/10.1002/maco.202213140

[3] R. Singh, D. Prasad, *Corrosion: Basics, economic adverse effects, and its mitigation, grafted biopolymers as corrosion inhibitors: Safety, Sustainability, Efficiency*, John Wiley & Sons. Inc., New York, USA, 2023, p. 1-10. https://doi.org/10.1002/9781119881391.ch1

[4] M. Ghazi Kadhim AlFalah, M. Saracoglu, M. I. Yilmazer, F. Kandemirli, Corrosion inhibition performance of 2- Fluorophenyl-2, 5-dithiohydrazodicarbonamide for copper in 3.5%NaCl Media: Experimental and Monte Carlo insights, *Al-Qadisiyah Journal for Engineering Sciences* **16** (2023) 150-159. https://doi.org/10.30772/qjes.2023.178995

[5] M. Ghazi, K. Alfalah, M. Izzettin, K. Saad, M. Freigita, Corrosion inhibition potential of new oxo-pyrimidine derivative on mild steel in acidic solution : Experimental and theoretical approaches, *Journal of Molecular Structure* **1315** (2024) 138773. https://doi.org/10.1016/j.molstruc.2024.138773

[6] A. A. Al-Amiery, W. N. R. W. Isahak, W. K. Al-Azzawi, Corrosion inhibitors: Natural and synthetic organic inhibitors, *Lubricants* **11** (2023) 174. https://doi.org/10.3390/lubricants11040174

[7] R. Aslam, G. Serdaroglu, S. Zehra, D.K. Verma, J. Aslam, L. Gui, C. Verma, E. E. Ebonso, M. A. Quraishi, Corrosion inhibition of steel using different families of organic compounds: Past and present progress, *Journal of Molecular Liquids* **348** (2022) 118373. https://doi.org/10.1016/j.molliq.2021.118373

[8] H. Assad, A. Kumar, Understanding functional group effect on corrosion inhibition efficiency of selected organic compounds, *Journal of Molecular Liquids* **344** (2021) 117755. https://doi.org/10.1016/j.molliq.2021.117755

[9] N. Arrousse, Y. Fernine, N. Al-Zaqri, A. Boshaala, E. Ech-chihbi, R. Salim, F. El Hajjaji, A. Alami, M. Ebn Touhami, M. Taleb, Thiophene derivatives as corrosion inhibitors for 2024-T3

aluminum alloy in hydrochloric acid medium, *RSC Advances* **12** (2022) 10321-10335. https://doi.org/10.1039/D2RA00185C

[10] K. Rasheeda, A. H. Alamri, P. A. Krishnaprasad, N. P. Swathi, V. D. P. Alva, T. A. Aljohani, Efficiency of a pyrimidine derivative for the corrosion inhibition of C1018 carbon steel in aqueous acidic medium: Experimental and theoretical approach, *Colloids and Surfaces A* **642** (2022) 128631. https://doi.org/10.1016/j.colsurfa.2022.128631

[11] Q. Zhang, L. Luo, H. Xu, Z. Hu, C. Brommesson, J. Wu, Z. Sun, Y. Tian, K. Uvdal, Design, synthesis, linear and nonlinear photophysical properties of novel pyrimidine-based imidazole derivatives, *New Journal of Chemistry* **40** (2016) 3456-3463. https://doi.org/10.1039/C5NJ02874D

[12] M. Yadav, S. Kumar, R. Sinha, I. Bahadur, E. E. Ebenso, New pyrimidine derivatives as efficient organic inhibitors on mild steel corrosion in acidic medium: Electrochemical, SEM, EDX, AFM and DFT studies, *Journal of Molecular Liquids* **211** (2015) 135-145. https://doi.org/10.1016/j.molliq.2015.06.063

[13] N. Arrousse, R. Salim, Y. Kaddouri, D. Zahri, F. El Hajjaji, R. Touzani, M. Taleb, S. Jodeh, The inhibition behavior of two pyrimidine-pyrazole derivatives against corrosion in hydrochloric solution: Experimental, surface analysis and in silico approach studies, *Arabian Journal of Chemistry* **13** (2020) 5949-5965. https://doi.org/10.1016/j.arabjc.2020.04.030

[14] K. Ansari, M. A. Quraishi, A. Singh, S. Ramkumar, I. B. Obot, Corrosion inhibition of N80 steel in 15% HCl by pyrazolone derivatives: Electrochemical, surface and quantum chemical studies, *RSC Advances* **6** (2016) 24130-24141. https://doi.org/10.1039/C5RA25441H

[15] C. Verma, M. A. Quraishi, Recent progresses in Schiff bases as aqueous phase corrosion inhibitors: Design and applications, *Coordination Chemistry Reviews* **446** (2021) 214105. https://doi.org/10.1016/j.ccr.2021.214105

[16] U. Nazir, Z. Akhter, N. K. Janjua, M. A. Asghar, S. Kanwal, T. M. Butt, A. Sani, F. Liagat, R. Hussain, F. U. Shah, Biferrocenyl Schiff bases as efficient corrosion inhibitors for an aluminium alloy in HCl solution: A combined experimental and theoretical study, *RSC Advances* **10** (2020) 7585-7599. https://doi.org/10.1039/C9RA10692H

[17] S. L. Granese, B. M. Rosales, C. Oviedo, J. O. Zerbino, The inhibition action of heterocyclic nitrogen organic-compounds on Fe and steel in HCl media, *Corrosion Science* **33** (1992) 1439-1453. https://doi.org/10.1016/0010-938X(92)90182-3

[18] K. F. Khaled, N. A. Al-Mobarak, Predictive model for corrosion inhibition of mild steel by thiophene and its derivatives using artificial neural network, *International Journal of Electrochemical Science* **7** (2012) 1045-1059. https://doi.org/10.1016/S1452-3981(23)13393-1

[19] Z. Atioğlu, H. Karataş, Z. Kökbudak, The crystal structure of 5-benzoyl-1-[(E)-(4-fluorobenzylidene) amino]-4-phenylpyrimidin-2 (1H)-one, $C_{24}H_{16}FN_3O_2$, *Zeitschrift für Kristallographie - New Crystal Structures* **236** (2021) 1035-1037. http://dx.doi.org/10.1515/ncrs-2021-0216

[20] M. J. Frisch, G. W. Trucks, H. B. Schlegel, G. E. Scuseria, M. A. Robb, J. R. Cheeseman, G. Scalmani, V. Barone, G. A. Petersson, H. Nakatsuji, X. Li, M. Caricato, A. Marenich, J. Bloino, B. G. Janesko, R. Gomperts, B. Mennucci, H.P . Hratchian, J. V. Ortiz, A. F. Izmaylov, J. L. Sonnenberg, D. Williams-Young, F. Ding, F. Lipparini, F. Egidi, J. Goings, B. Peng, A. Petrone, T. Henderson, D. Ranasinghe, V. G. Zakrzewski, J. Gao, N. Rega, G. Zheng, W. Liang, M. Hada, M. Ehara, K. Toyota, R. Fukuda, J. Hasegawa, M. Ishida, T. Nakajima, Y. Honda, O. Kitao, H. Nakai, T. Vreven, K. Throssell, J. A. Montgomery, Jr., J. E. Peralta, F. Ogliaro, M.

Bearpark, J. J. Heyd, E. Brothers, K .N. Kudin, V. N. Staroverov, T. Keith, R. Kobayashi, J. Normand, K. Raghavachari, A. Rendell, J. C. Burant, S. S. Iyengar, J. Tomasi, M. Cossi, J. M. Millam, M. Klene, C. Adamo, R. Cammi, J. W. Ochterski, R. L. Martin, K. Morokuma, O. Farkas, J.B. Foresman, D. J. Fox, Gaussian, Inc., Wallingford CT, 2016., https://gaussian.com/citation/

[21] G. Gece, The use of quantum chemical methods in corrosion inhibitor studies, *Corrosion Science* **50** (2008) 2981-2992. https://doi.org/10.1016/j.corsci.2008.08.043

[22] G. Gece, S. Bilgiç, Quantum chemical study of some cyclic nitrogen compounds as corrosion inhibitors of steel in NaCl media, *Corrosion Science* **51** (2009) 1876-1878. https://doi.org/10.1016/j.corsci.2009.04.003

[23] M. G. K. Alfalah, A. H. Abbar, F. Kandemirli, Improving the corrosion behaviour of Zn-Ni alloy coatings on 316 SS from chloride-sulfate bath by addition of triethanolamine or sucrose, *Journal of Electrochemical Science and Engineering* **15** (2025) 2607. https://doi.org/10.5599/jese.2607

[24] M. G. K. AlFalah, K. S. M. Freigita, M. I. Yilmazer, M. Saracoglu, Z. Kokbudak, F. Kandemirli, Corrosion inhibition potential of new oxo-pyrimidine derivative on mild steel in acidic solution: Experimental and theoretical approaches, *Journal of Molecular Structure* **1315** (2024) 1-13. https://doi.org/10.1016/j.molstruc.2024.138773

[25] Ž. . Tasić, M. B. Petrović Mihajlović, M. B. Radovanović, A. T. Simonović, M. M. Antonijević, Cephradine as corrosion inhibitor for copper in 0.9% NaCl solution, *Journal of Molecular Structure* **1159** (2018) 46-54. https://doi.org/10.1016/j.molstruc.2018.01.031

[26] M.A . Amin, S. S. Abd El-Rehim, E. E. F. El-Sherbini, R. S. Bayoumi, The inhibition of low carbon steel corrosion in hydrochloric acid solutions by succinic acid, *Electrochimica Acta* **52** (2007) 3588-3600. https://doi.org/10.1016/j.electacta.2006.10.019

[27] M. G. K. AlFalah, E. Kamberli, A. H. Abbar, F. Kandemirli, M. Saracoglu, Corrosion performance of electrospinning nanofiber ZnO-NiO-CuO/polycaprolactone coated on mild steel in acid solution, *Surfaces and Interfaces* **21** (2020) 100760. https://doi.org/10.1016/j.surfin.2020.100760

[28] C. Verma, I. B. Obot, I. Bahadur, E. S. M. Sherif, E. E. Ebenso, Choline based ionic liquids as sustainable corrosion inhibitors on mild steel surface in acidic medium: Gravimetric, electrochemical, surface morphology, DFT and Monte Carlo simulation studies, *Applied Surface Science* **457** (2018) 134-149. https://doi.org/10.1016/j.apsusc.2018.06.035

[29] M. Evecen, Alfalah, M. G. K, Improvement of the corrosion behaviour of mild steel by deposition of Zn-Ni-Cu-Fe-Cd from an acetate sulphate bath, *Ochrona Przed Korozja* **1** (2025) 9-15. https://doi.org/10.15199/40.2025.2.2

[30] M. Murmu, S. K. Saha, P. Bhaumick, N. C. Murmu, H. Hirani, P. Banerjee, Corrosion inhibition property of azomethine functionalized triazole derivatives in 1 mol.L−1 HCl medium for mild steel: Experimental and theoretical exploration, *Journal of Molecular Liquids* **313** (2020) 113508. https://doi.org/10.1016/j.molliq.2020.113508

[31] K. S. M. Ferigita, M. G. K. AlFalah, M. Saracoglu, Z. Kokbudak, S. Kaya, M. O. A. Alaghani, F. Kandemirli, Corrosion behaviour of new oxo-pyrimidine derivatives on mild steel in acidic media: Experimental, surface characterization, theoretical, and Monte Carlo studies, *Applied Surface Science* **7** (2022) 100200. https://doi.org/10.1016/j.apsadv.2021.100200

[32] M. G. K. AlFalah, F. Kandemirli, Corrosion inhibition potential of dithiohydrazodicarbonamide derivatives for mild steel in acid media: Synthesis,

experimental, DFT, and Monte Carlo studies, *Arabian Journal for Science and Engineering* **47** (2022) 6395-6424. https://doi.org/10.1007/s13369-021-06368-y

[33] A.Y. Musa, A. A. H. Kadhum, A. B. Mohamad, A. A. B. Rahoma, H. Mesmari, Electrochemical and quantum chemical calculations on 4,4-dimethyloxazolidine-2-thione as inhibitor for mild steel corrosion in hydrochloric acid, *Journal of Molecular Structure* **969** (2010) 233-237. https://doi.org/10.1016/j.molstruc.2010.02.051

[34] A. Popova, M. Christov, T. Deligeorgiev, Influence of the molecular structure on the inhibitor properties of benzimidazole derivatives on mild steel corrosion in 1 M hydrochloric acid, *Corrosion* **59** (2003) 756-764. https://doi.org/10.5006/1.3277604

[35] C. Verma, E. E. Ebenso, M. A. Quraishi, Ionic liquids as green and sustainable corrosion inhibitors for metals and alloys: An overview, *Journal of Molecular Liquids* **233** (2017) 403-414. https://doi.org/10.1016/j.molliq.2017.02.111

[36] R. Yıldız, An electrochemical and theoretical evaluation of 4,6-diamino-2-pyrimidinethiol as a corrosion inhibitor for mild steel in HCl solutions, *Corrosion Science* **90** (2015) 544-553. https://doi.org/10.1016/j.corsci.2014.10.047

[37] J. Bhawsar, P. Jain, M. G. Valladares-Cisneros, C. Cuevas-Arteaga, M. R. Bhawsar, Quantum chemical assessment of two natural compounds: Vasicine and vasicinone as green corrosion inhibitors, *International Journal of Electrochemical Science* **13** (2018) 3200-3209. https://doi.org/10.20964/2018.04.57

[38] L. C. Murulana, A. K. Singh, S. K. Shukla, M. M. Kabanda, E. E. Ebenso, Experimental and quantum chemical studies of some bis(trifluoromethyl-sulfonyl). Imide imidazolium-based ionic liquids as corrosion inhibitors for mild steel in hydrochloric acid solution, *Journal of Industrial and Engineering Chemistry* **51** (2012) 13282-13299. https://doi.org/10.1021/ie300977d

[39] Y. El Aoufir, R. Aslam, F. Lazrak, R. Marzouki, S. Kaya, S. Skal, A. Ghanimi, I. H. Ali, A. Guenbour, H. Lgaz, I. M. Chung, The effect of the alkyl chain length on corrosion inhibition performances of 1,2,4-triazole-based compounds for mild steel in 1.0 M HCl: Insights from experimental and theoretical studies, *Journal of Molecular Liquids* **303** (2020) 112631. https://doi.org/10.1016/j.molliq.2020.112631

[40] N. A. Wazzan, I. B. Obot, S. Kaya, Theoretical modelling and molecular level insights into the corrosion inhibition activity of 2-amino-1,3,4-thiadiazole and its 5-alkyl derivatives, *Journal of Molecular Liquids* **221** (2016) 579-602. https://doi.org/10.1016/j.molliq.2016.06.011

[41] S. Kaya, C. Kaya, L. Guo, F. Kandemirli, B. Tüzün, İ. Uğurlu, L.H. Madkour, M. Saraçoğlu, Quantum chemical and molecular dynamics simulation studies on inhibition performances of some thiazole and thiadiazole derivatives against corrosion of iron, *Journal of Molecular Liquids* **219** (2016) 497-504. https://doi.org/10.1016/j.molliq.2016.03.042

[42] L. Guo, S. Zhu, S. Zhang, Q. He, W. Li, Theoretical studies of three triazole derivatives as corrosion inhibitors for mild steel in acidic medium, *Corrosion Science* **87** (2014) 366-375. https://doi.org/10.1016/j.corsci.2014.06.040

[43] R. Hasanov, M. Sadıkoğlu, S. Bilgiç, Electrochemical and quantum chemical studies of some Schiff bases on the corrosion of steel in H_2SO_4 solution, *Applied Surface Science* **253** (2007) 3913-3921. https://doi.org/10.1016/j.apsusc.2006.08.025

[44] P. K. Chattaraj, B. Maiti, Reactivity dynamics in atom−field interactions: A quantum fluid density functional study, *The Journal of Physical Chemistry A* **105** (2001) 169-183. https://doi.org/10.1021/jp0019660

[45] C. Verma, M. A. Quraishi, K. Kluza, M. Makowska-Janusik, L. O. Olasunkanmi, E. E. Ebenso, Corrosion inhibition of mild steel in 1 M HCl by D-glucose derivatives of dihydropyrido [2,3-d:6,5-d'] dipyrimidine-2, 4, 6, 8 (1H,3H,5H,7H)-tetraone, *Scientific Reports* **7** (2017) 44432. https://doi.org/10.1038/srep44432

[46] G. Gao, C. Liang, Electrochemical and DFT studies of β-amino-alcohols as corrosion inhibitors for brass, *Electrochimica Acta* **52** (2007) 4554-4559. https://doi.org/10.1016/j.electacta.2006.12.058

[47] R. G. Parr, L. V. Szentpály, S. Liu, Electrophilicity index, *Journal of the American Chemical Society* **121** (1999) 1922-1924. https://doi.org/10.1021/ja983494x

[48] M. Djenane, S. Chafaa, N. Chafai, R. Kerkour, A. Hellal, Synthesis, spectral properties and corrosion inhibition efficiency of new ethyl hydrogen [(methoxyphenyl) (methylamino) methyl] phosphonate derivatives: Experimental and theoretical investigation, *Journal of Molecular Structure* **1175** (2019) 398-413. https://doi.org/10.1016/j.molstruc.2018.07.087

[49] M. A. Quraishi, R. Sardar, Hector bases - a new class of heterocyclic corrosion inhibitors for mild steel in acid solutions, *Journal of Applied Electrochemistry* **33** (2003) 1163-1168. https://doi.org/10.1023/B:JACH.0000003865.08986.fb

[50] H. Tanak, A. Ağar, M. Yavuz, Experimental and quantum chemical calculational studies on 2-[(4-fluorophenylimino) methyl]-3,5-dimethoxyphenol, *Journal of Molecular Modeling* **16** (2010) 577-587. https://doi.org/10.1007/s00894-009-0574-2

[51] A. Tazouti, M. Galai, R. Touir, M. E. Touhami, A. Zarrouk, Y. Ramli, M. Saracoglu, S. Kaya, F. Kandemirli, C. Kaya, Experimental and theoretical studies for mild steel corrosion inhibition in 1.0 M HCl by three new quinoxalinone derivatives, *Journal of Molecular Liquids* **221** (2016) 815-832. https://doi.org/10.1016/j.molliq.2016.03.083

[52] M. Shahraki, M. Dehdab, S. Elmi, Theoretical studies on the corrosion inhibition performance of three amine derivatives on carbon steel: Molecular dynamics simulation and density functional theory approaches, *Journal of the Taiwan Institute of Chemical Engineers* **62** (2016) 313-321. https://doi.org/10.1016/j.jtice.2016.02.010

[53] D. Bhattacharjee, T. K. Devi, R. Dabrowski, A. Bhattacharjee, Birefringence, polarizability order parameters and DFT calculations in the nematic phase of two bent-core liquid crystals and their correlation, *Journal of Molecular Liquids* **272** (2018) 239-252. https://doi.org/10.1016/j.molliq.2018.09.052

[54] N. V. Likhanova, M. A. Domínguez-Aguilar, O. Olivares-Xometl, N. Nava-Entzana, E. Arce, H. Dorantes, The effect of ionic liquids with imidazolium and pyridinium cations on the corrosion inhibition of mild steel in acidic environment, *Corrosion Science* **52** (2010) 2088-2097. https://doi.org/10.1016/j.corsci.2010.02.030